A Quantum Information Processing Machine for Computing by Observables

F. Remacle[1,2], R. D. Levine[2,3*]

[1] Theoretical Physical Chemistry, University of Liège, 4000 Liège, Belgium
[2] The Fritz Haber Research Center for Molecular Dynamics, The Hebrew University of Jerusalem, 91904 Jerusalem, Israel
[3] Department of Chemistry and Biochemistry and Department of Molecular and Medical Pharmacology, David Geffen School of Medicine, University of California, Los Angeles, CA 90095, USA

Key words: Coherences as logic variables; Semiconducting colloidal quantum dots; quantum information processing; 2D electronic spectroscopy; Lie algebraic dynamics; Singular value decomposition

*Corresponding author: Raphael Levine, Raphy@mail.huji.ac.il

Abstract (222 words)

A quantum machine that accepts an input and processes it in parallel is described. The logic variables of the machine are not wavefunctions (qubits) but observables (i.e., operators) and its operation is described in the Heisenberg picture. The active core is a solid-state assembly of small nanosized colloidal quantum dots (QDs) or dimers of dots. The size dispersion of the QDs that causes fluctuations in their discrete electronic energies is a limiting factor. The input to the machine is provided by a train of very brief laser pulses, at least four in number. The coherent band width of each ultrashort pulse needs to span at least several and preferably all the single electron excited states of the dots. The spectrum of the QD assembly is measured as a function of the time delays between the input laser pulses. The dependence of the spectrum on the time delays can be Fourier transformed to a frequency spectrum. This spectrum of a finite range in time is made up of discrete pixels. These are the visible, raw, basic logic variables. The spectrum is analyzed to determine a possibly smaller number of principal components. A Lie-algebraic point of view is used to explore the use of the machine to emulate the dynamics of other quantum systems. An explicit example demonstrates the considerable quantum advantage of our scheme.

Significance statement (100 words)

Principles of operation of a quantum machine that can emulate the dynamics of other quantum systems are described. The logic variables are the populations and coherences of N in number excited states of ultrafast pumped small colloidal quantum dots. A Lie algebraic construction shows that the machine can process up to N^2 variables. The transition from N to N^2 variables is the quantum advantage. (The observables that are our logic variables are *bi*linear in the N wave functions). A singular value decomposition can identify the dominant observables that govern the logic processing. Explicit analytical results for N^2=9 observables are provided.

Introduction

Ultrafast spectroscopy is a major direction to novel quantum technologies.(1, 2) Quantum nonlinear spectroscopy (3) offers many ways to control quantum systems and to take advantage of the superposition that is inherent to quantum dynamics.(4) An extensively used nonlinear technique is the two dimensional, 2D, spectroscopy that was first explored in the infrared and has since been usefully applied in the UV. (2, 5-10) It is an ultrafast technique because the light pulses used must be short enough that their coherent width in energy can cover the span of several quantum states. Thereby one can prepare a coherent superposition of states. Experimentally it is now recognized that even in the UV the coherence in 2D electronic spectroscopy (2DES) can survive for more than a few periods of fast beating electronic coherences, with periods as short as a dozen of fs.(2) There is therefore a time window where the electronic degrees of freedom are not yet effectively coupled to the intrasystem vibrations and neither to the environment. Any loss of coherence is then primarily inhomogeneous in origin. 2D spectroscopy has done much towards the understanding of the dynamics of proteins and other larger molecules that are of interest in biology.(11, 12) Inorganic systems that have a higher density of electronic states in the visible and near UV are quantum dots (QD).(13-15) We specifically mean colloidal quantum dots that are molecular systems prepared by chemical means, systems whose mean size can be small, say a very few nanometers. The price for this small size is the dispersion in size which, when limited, is the main source of inhomogeneous dephasing of the coherence of an ensemble of dots.(16)

The design that we discuss has an essential difference from the more canonical formulations of quantum computing(17) and/or quantum machine learning.(18-20) The familiar quantum gates operate on wave functions. The elementary unit is a qubit, a linear combination of two quantum states. A Qudit is a coherent combination of several states.(21-23) Here we work with observables, typically Hermitian operators that are said to live in Liouville space(24) unlike wave functions whose habitat is the Hilbert space. Very early on, Dirac established the equivalence of the two descriptions. We shall try to highlight the advantage of designing with observables. Of course, for such applications where a wave function description is currently very highly refined such as in quantum chemistry, computing an electronic wave function is a highly worth-while goal. This is so even when we recognize that typically a wave function contains much too much detail than needed for determining the usual observable properties. There is also the very practical aspect of the enormous resources needed to store a wave function for a not small many body system let

alone a protein. For people interested in dynamics and in a time dependent view of spectroscopy (1, 3, 25, 26) an approach based on the Heisenberg picture dynamics of observables can be of more direct interest. In particular because at very short times only a much more limited number of states needs to be considered.

We here examine in detail the spectral maps that are generated by 2D electronic spectroscopy of small quantum dots and dimers of small dots. There is combined experimental and theoretical evidence that for small few nm QDs connected by small sub nanometric linkers there is coherent coupling between the two QDs in the dimer. (13-15, 27) We envisage a BoxCARS(2, 6) geometry to describe the experiment because it is simpler and sufficient for our purpose. There are clear advantages for using action detection such as fluorescence(28) or photocurrents(29-31) and for using a larger number of laser pulses (6, 8 or even more) as compared to the four pulses that are used in current 2DES scheme. However, we mean to demonstrate that already the currently available approach offers what we ultimately seek namely to claim that the hardware combined with a 2DES set-up can act as a quantum computer in the original sense of Feynman.(32)

We have two central technical aims. The first is to characterize the spectral maps produced by the QD assemblies that are used in the actual device.(13-15, 27) This is analogous to seeking to determining the process matrix in the sense of Yuen-Zhou et al.(1, 33) The fast dephasing of the excited states means that experimentally one is limited to having only the ground electronic state of the dots as an initial state. So we can determine a row of the process matrix. The 2D experimental results of our hardware are conveniently represented as spectral maps, Figure 1. The polarization of the density matrix is measured for a series of values of the time intervals, T_1, T_2, T_3, between the four laser pulses. A spectral map is the polarization at a series of time points T_2 where the two axis are the Fourier transform of time intervals T_1 and T_3. (1, 33, 34) We begin by first vectorizing the maps at a sequence of time points along the T_2 axis, see Figure 1. Each map is thereby converted to a column of an 'overall' matrix representing the entire output. We can achieve a major compaction of the experimental results by performing a singular value decomposition, SVD, on the overall matrix and retaining only the more major components.

Our second central aim is to show how the dynamics of the hardware enables us to compute or, strictly speaking, to emulate, the dynamics of a different, other, quantum system. This targeted system is the system of interest. There are, of course, limitations. First and foremost the (finite) size of the Hilbert space in which the system of interest is specified needs to be smaller or equal

to the size, *N*, of the Hilbert space that is sufficient to describe the (short time) dynamics of the hardware. Of course, we need to specify the system of interest and for this purpose we will require the finite spectrum of its Hamiltonian or a set of operators (= the observables) that is closed under commutation with one another and with the Hamiltonian. See refs.(35, 36) for simple concrete examples. In our Hilbert space a sufficient set of operators that meet both requirements is the set of Gelfand projectors, E_{ij}, that are represented as *N* by *N* matrices where all entries are zero except in the row *i* and column *j* where the value is unity. *N* is the size of the relevant Hilbert space and any matrix representing an observable in this Hilbert space can be written as a linear combination of these N^2 Gelfand matrices.. For the theorist, the maps produced by the 2D spectroscopy are *N* by *N* matrices with entries, the polarizations, see below, that are complex numbers. Similarly the outputs of the emulation of the system of interest are such matrices. To make these comments more concrete we begin by discussing the hardware and its spectroscopy as determined by the 2D experimental scheme. This will bring forward the point that for the experimentalists the maps produced by the 2DES are typically larger than the *N* by *N* matrices of the theorist. The entries in the directly observed experimental maps are the intensities observed after Fourier transforming the emitted signal as a function of time intervals to frequency axes, see figure 1 below. The overall range in time of the intervals determines the width in frequency of the individual pixels while the spacing in time points determines the number of pixels along a frequency axis. Typically there are many more than N^2 pixels in any experimental 2D frequency map. For a theorist, a map of a physical system at a given time is an *N* by *N* matrix. As is discussed in detail below, the larger number of pixels that is addressed can be made into an advantage in that several different initial states for the emulation can be prepared in just one experiment.

The Spectroscopy of the Hardware

The 2D electronic spectroscopy of the hardware has been realized experimentally.(13, 15, 27) It is an assembly of dimers where each dimer is two coherently coupled quantum dots. The number *N* is the number of one photon excited states of the dimer that are accessible from the ground state, GS. See (14, 16) for concrete examples and details. These one-photon excited states are sometimes called, by analogy, excitons. We here deal exclusively with monoexcitons but towards achieving higher information processing and storage capabilities it can be of interest to access also higher, (biexciton etc.), excited states. The essence of the input and its processing are shown in figure 1.

The 2D electronic spectroscopy as discussed here is performed in a BoxCARS geometry using a sequence of three short fs laser pulses that are not overlapping in time, figure 1. Sometimes one omits to mention a fourth pulse, a local oscillator, that induces light emission at the time *t* after the start of the experiment when the system was in its ground electronic state. The time *t* is the time along which the dynamics evolve. The experiment is often discussed in terms of the time intervals between the laser pulses as shown in figure 1, so that the time *t* is given by $t = T_0+T_1+T_2+T_3$.

In the simple case of a single monoexciton band and one photon transitions, the observed polarization is the emission to the ground state. It is given as the expectation value over the density matrix at the time *t* of the transition dipole moment $\hat{\mu}$ between the *N* excited states and the ground state: The dipole operator $\hat{\mu}$ of interest here is the operator that induces emission only from the *N* excited states $\left\{\left|m\right\rangle, m=1,2,..,N\right\}$ $\left\{\left|m\right\rangle, m=1,2,..,N\right\}$ to the GS and is therefore of the form

$$\hat{\mu} = \sum_{m=1}^{N} \mu_{GS-m} \left|GS\right\rangle\left\langle m\right| \qquad (1)$$

This is because in the set-up as discussed, the carrier frequency of the pulses is roughly one photon resonant with the monoexcitons and the duration of the pulse is such that several monoexcitons fall within its coherent energy bandwidth.

The density matrix up to time *t* is:

$$\hat{\rho}(t) = \sum_{k,m} \rho_{km}(t) \left|k\right\rangle\left\langle m\right| \qquad (2)$$

Only a small submatrix of this $\hat{\rho}(t)$ is probed by the emission to the ground state. It is the submatrix where the *N* excited states, $m = 1, ..., N$ emit to the ground state, k = GS. Note an essential fact, not explicit in the notation in equation (2), that the density matrix implicitly depends on the coherences between the excited states. This will be clear when one explicitly shows the dependence on the time interval T_2.

For a given triplet of time intervals T_1, T_2, T_3 , see figure 1, one can express the polarization of the emission, as

$$P_{T_1,T_2,T_3}(t) = \mathrm{Tr}\left[\hat{\mu}\hat{\rho}(t)\right] = \sum_{l=1}^{N} \rho_{GS-l}^{T_1T_2T_3}(t)\mu_{l-GS} \qquad (3)$$

$P_{T_1T_2T_3}(t)$ is a complex number and the emitted field is proportional to $iP_{T_1T_2T_3}(t)$. In 2DES, the polarization signal at a given time interval T_2 is conveniently represented as a 2D discrete map namely a matrix where the axis or equivalently the matrix elements are indexed by the intervals T_1 and T_3. One can then assemble the matrices for different values of T_2 into a tensor with elements indexed by the three time intervals, T_1, T_2, T_3, see Figure 1. Our notation above reflects the physical result that the density matrix depends not only on the actual value of the time *t* but also on how the sum *t* is made up in terms of the triplet of times, T_1, T_2, T_3.

To interpret a pixel of a 2D map at a particular triplet T_1, T_2, T_3 it is often convenient to use third order perturbation theory.(1, 34) Each matrix, which is at a given value of T_2, is typically plotted after a Fourier transform along the T_1 and T_3 axes and is thereby a matrix indexed by the frequencies ω_1 and ω_3, see Figure 1. In the ideal case of well-resolved excited states the peaks in the maps are at the frequencies ω_1 and ω_3 that are the energies of the excited states in atomic units $\hbar = 1$. As we vary T_2 each peak in the ideal case has the phase

$$\vartheta_{ij} = \exp\left((\omega_{1i} - \omega_{3j})t\right) \tag{4}$$

corresponding to the coherence between the two excited states *i* and *j* at a particular time *t*. The energies of the dots depend on their size so when there is a not negligible size disorder, the resulting inhomogeneous broadening means that there can be coherences that beat in more than one given pixel on the frequency map. The number of excited states that contribute to the response, *N,* can therefore be smaller than the number of pixels, N_p (which is determined by the sampling along T_1 and T_3). The analysis of the beating periods along T_2 can be done by performing a third FT along T_2.(15, 37) However, this is not the most stable method and can possibly result in artifacts.

Intermezzo: A simple example of quantum computing with the hardware

We aim for diverse applications of the hardware towards quantum computing. Here is a preliminary report of a very simple and elementary but quite explicit application to the quantum vibrational dynamics of a linear triatomic molecule. This extends our earlier work(35, 36) in that here we do not need the vibrations to be harmonic although it does lead to a simpler procedure when they are. The two vibrational coordinates are described on a discrete square grid with small

spacings along the bond distances. A map of the amplitude of the vibrational wave function of the molecule on different grid points at a given time is mathematically equivalent to a spectral map of a 2D spectrum at a given time T_2. Instead of using localized basis function as needed for a DVR (38) one can expand the wave fuction of the molecule in other basis states, e.g., eigenfunctions of a useful zeroth order Hamiltonian. Here too, for two coupled vibrations a map of the amplitude of the wave function on different basis functions at a given time is mathematically equivalent to a spectral map of a 2D spectrum at a given time T_2.

To simulate time change we start with an initial non stationary state of the molecule that is represented by the spectral map at a time shortly after the second pulse is over. The subsequent dynamics occur along the T_2 time axis. We distinguish between harmonic and anharmonic vibrations. In the harmonic case there are three frequencies and typically these can be matched or nearly so with frequencies of coherences in the hardware. So the evolution along T_2 is readily accounted for as shown in our earlier work.(35, 36) Otherwise, and for anharmonic vibrations, we need to stretch or squeeze segments along the axis of T_2 so the phase change of the time evolving vibrations matches the phase changes of the coherences due to the different spacings provided by the electronic excitonic manifold of the hardware. This phase matching is covered in more detail by the complementary analysis using the variable projection approach.(39) The SVD procedure can be extended to more than two dimensions(40) and so the dynamics of more coupled vibrations can be emulated.

Characterizing the spectral maps of the hardware

We use the well documented(41, 42) singular value decomposition, SVD, as a way to characterize the *entire* spectral output of the hardware in one expression. To do so we first generate a matrix **A** where each row is a vector labelled by a particular time interval T_2, see figure 1(c). The $N_p = N_{T_1}$ by N_{T_3} elements of the vector are the observed intensities at each pixel such that the row is a vectorized form of the 2D spectral matrix at that time T_2. N_{T_1} and N_{T_3} are the number of times sampled along T_1 and T_3 respectively. The matrix **A**, figure 1(c), is rectangular with dimensions N_p by N_{T_2} where N_{T_2} is the number of points samples along T_2. One needs to sample T_2 to long times to uncover all the periods of the coherences between excited states. So in

general $N^2 < N_p$ and we take it that $N_p > N_{T_2}$. The SVDecomposition of **A** is the matrix product $\mathbf{A} = \mathbf{USV}^\dagger$ or, explicitly, for the matrix element at the *i*'th row, a pixel index, meaning that *i* is the double index ω_1, ω_3 and the column, a time t_k along T_2.

$$\left(\mathbf{A}\right)_{it_k} = \sum_{\alpha=1}^{M} U_{i\alpha} S_\alpha V^*_{t_k\alpha} = \sum_{\alpha=1}^{M} \lambda_{\alpha t_k} U_{i\alpha} \qquad (5)$$

Here S_α is a singular value, an element of the diagonal matrix **S** and in the notation of surprisal analysis(43) $\lambda_{\alpha t_k} = S_\alpha V^*_{t_k\alpha}$ is a time dependent multiplier, the weight of the component α at the time t_k. $U_{i\alpha}$ is a time independent element of the constraint α giving the weight of pixel *i* in that constraint. *M* is the number of terms in the SVDecomposition. To get an exact representation, one needs to include $M = N_{T_2}$ terms. We rank the terms in the sum in decreasing order of the singular values S_α. The inevitable experimental noise means that the constraints with lower values of the S_α's are the more corrupted by noise and so the sum is often truncated keeping far fewer terms than N_{T_2} and thereby providing a very compact representation for the matrix **A** which is the matrix representing the entire output of the harware.

To keep only the number of eigenvalues above noise, Shrager(44) suggests computing the autocorrelation function of the normalized eigenvectors **V** and **U**.

Example: a SVD decomposition of a model hardware.

We model an ensemble of dimers of small CdSe dots with 5% disorder in size of the dots. The details of the electronic states of the dimer are given in much detail in our two earlier papers(35, 36) and in their supplementray information files in particular. The essence is that the 24 states in the first excited, monoexitonic band of the monomer are clustered in four bands of states as shown in figure 2. In the dimer the four monomer bands that couple to eight bands as shown. The 2D spectrum is generated as described (36) with $N_{T_1} = N_{T_3}$ =200 points for ω_1 and for ω_3 generating N_p = 40,000 pixels. The spectrum is that of an multilayered assembly of dimers and because of the finite size dispersion each coherence address in the (ω_1, ω_3) plane is broadened to a cloud of

nearby points as described.(16) The SVD analysis reported below is done on the real part of the maps. We find 10 significant singular values S_α that come roughly by pairs, see figure 2.

The largest component identified by SVD shows the most intense diagonal population peak (the brightest S_1 band of the dimer, it is the highest one, the lowest one should be dark if we had no size dispersion). The 4 next eigenvalues correspond to coherences between states of the S_1 and S_2 bands. The next 2 correspond to the coherences between the two bands of the split S_1 band of the dimer (the highest one is brighter than the lowest one), and we have a longer period ≈ 30 fs. All together SVD provides important 4 pairs of coherences in addition of the two largest singular values, that are population peaks, to get a good description of the input maps.

The dominant observables

The SVD derived eigenvector $U_{i\alpha}$ is the weight relation between the visible pixel *i* to the invisible component α. The importance of this connection at the time t_k is given by the time dependent weight $\lambda_{\alpha t_k} = S_\alpha V^*_{t_k \alpha}$. The singular value S_α determines the overall importance of the component while $V_{t_k \alpha}$ is fractional importance at the time t_k. The M invisible components identified by the SVD, equation (5), $\left(\mathbf{A}\right)_{it_k} = \sum_{\alpha=1}^{M} U_{i\alpha}\lambda_{\alpha t_k}$ reproduce the readout at pixel *i* at that time. The steep drop of the singular values for $\alpha > M$, figure 2, means that the reproduction with M = 10 is accurate for our hardware model. Keeping all the N_{T_2} singular values provides a mathematically exact reproduction.

The initial state

For the purpose of computing, the input to the machine is provided by the first two lasers. The initial state is the map A at a very short time after T_2 = 0 just so that the second short laser pulse is already negligible. Along a frequency axis of the map, there are more pixels than quantum states, $N_{T_1}, N_{T_3} > N$. Therefore the machine could process more than one initial state at a time.

The dynamics is linear, a key advantage, thereby the machine not only processes a given state in parallel(34) it also is capable of processing different initial states in parallel. This leaves open

the practical issue of how to resolve the observed large matrix of pixels as a linear combination of independent but smaller N by N maps.

Dynamics of a coherence $\left\langle \hat{E}_{ij} \right\rangle$ as a function of time along the T_2 axis

We aim to discuss the coherences and their evolution along the T_2 axis for the general case of an *N* level system. When *H* is the Hamiltonian of the unperturbed hardware then each coherence oscillates along T_2 with its own frequency, equation (4) for example. We discuss the more general case because we aim to examine the result how the coherences of the hardware can be used for emulating the coherences of the system that we wish to emulate, that evolve according to a different Hamiltonian. We will show that we can relate the two time evolutions so that in principle we show how to transform the dynamics of the system we need to emulate to the model spectral matrix of the hardware.

The first restriction that we impose is that the system to be emulated is described realistically in the same *N* dimensional Hilbert space, just like the hardware. Of course, using just *N* electronic excited states of the hardware and forgetting for example the phonons means that we provide a description of the hardware valid only for a short time interval after excitation. But all that we need is a description valid before dephasing seriously sets in and it is typically the size disorder that limits this time range. For the system to be emulated it may be that *N* states are all that we really need, see (35, 36) for example. In a Lie algebraic approach it is sufficient when we identify N^2 (or fewer) generators that are closed under commutation with the Hamiltonian.

To a Hamiltonian there corresponds a Liouvillian, *L*, a 'super operator' that acts on operators as $\left[H, \right]$ thereby generating the motion in time in the Heisenberg picture. Writing $\exp(iLt)$ as the form of the evolution super operator acting on the $\mathbb{N} \equiv N^2$ operators we have that the coherences in any orthonormal basis *i,j* at a time t_k along T_2 is given as

$$\hat{E}_{ij}(t) = \sum_{kl=1}^{\mathbb{N}} \left(\exp\left(i\mathbf{L}t_k \right) \right)_{ij,kl} \hat{E}_{kl}(0) \qquad (6)$$

The Liouvillian L in equation (6) corresponds to the Hamiltonian of the hardware and it is time-independent during the time interval T_2 along which the output os measured.

Computing by observables

We take it that the same set of $\mathbb{N} = N^2$ observables $\left\{ \hat{X}_i \right\}$ is used to describe the hardware and the target system that we wish to emulate. For the hardware that we use, the observables $\hat{X}_i$'s are

coherences (and populations) so that *i* is a double index, say $\alpha,\beta:\ \hat{X}_i \equiv \hat{E}_{\alpha\beta}$. In principle however, all that we require is that the observables close a Lie algebra:

$$\left[\hat{X}_j,\hat{X}_i\right]=\sum_k^{\mathbb{N}} C_{ji}^k \hat{X}_k \tag{7}$$

Equation (7) is naturally satisfied for the Gelfand set of observables.

$$\left[\hat{E}_{\alpha\beta},\hat{E}_{\gamma\delta}\right]=\hat{E}_{\alpha\delta}\delta_{\beta\gamma}-\hat{E}_{\gamma\beta}\delta_{\delta\alpha} \tag{8}$$

but it is sometimes possiblle to determine a closed algebra with a smaller number of operators. As discussed above, using SVD it is possible to identify a smaller swet of constraints that dominate the dynamics.

The Hamiltonian of the target system that we wish to emulate is taken to be a linear combination of the $\mathbb{N}$ observables in our set. This is inherently satisfied when we work in a finite dimensional Hilbert space where any matrix and therefore also the Hamiltonian matrix can be generated as

$$\hat{H}=\sum_i^{\mathbb{N}} h_i\hat{X}_i \tag{9}$$

For a closed set of obervables, equation (7), the equations of motion of the observables are therefore closed

$$i\hbar\frac{d\hat{X}_j}{dt}=\left[\hat{X}_j,\hat{H}\right]=\left[\hat{X}_j,\sum_i h_i\hat{X}_i\right]=\sum_i h_i\sum_k C_{ji}^k\hat{X}_k=\sum_k\hat{X}_k\sum_i C_{ji}^k h_i \tag{10}$$

Only the possibly time dependent coefficient $\{h_i\}$ is special to the target system that we wish to emulate. The equation factorizes the equation of motion as is further shown in equation (12)below. We rewrite equation (10) as a scalar product of an N^2 by N^2 matrix where $\mathbf{M}_j=\left\{C_{ji}^k\right\}$ is a matrix of structure constants relevant to taking the operation $\left[\hat{X}_j,\ \right]$ that is often denoted as adX_j. Note that the operators are bilinear in the wavefunctions so that their index such as *j* is actually two labels. When the operators are coherences the structure constants are immediate, so that for $j\equiv j_1,j_2$

$$\left(\mathbf{M}_j\right)_{ki}=\left[\left|j_1\right\rangle\left\langle j_2\right|,\left|a\right\rangle\left\langle b\right|\right]=\delta_{j_2,a}\left|j_1\right\rangle\left\langle b\right|-\delta_{j_1,b}\left|a\right\rangle\left\langle j_2\right| \tag{11}$$

In the supplementary information, SI, file we exhibit matrices $\mathbf{M}_j$ for different realizations of SU(2) and SU(3) algebras. Why do we sometimes use other than the coherences for the Lie algebra

- because there are many advantages when the observables are Hermitian and orthogonal. In terms of the matrix **M** we write equation (10) as

$$i\hbar\frac{dX_j}{dt}=\left[X_j,H\right]\equiv\sum_k L_{jk}X_k=\sum_i h_i\sum_k C_{ji}^k X_k=\left(\mathbf{h}^T\mathbf{M}_j\right)\cdot\mathbf{X} \tag{12}$$

The factorization, equation (12), is a key result. The point in the factorization is that the structure constants C_{ji}^k are common to the hardware and the target system while the coefficients *h* in the expansion of the Hamiltonian, equation (9), are different for the hardware and the system to be emulated.

Taking the expectation value of both sides of equation (10) on the density matrix, cf. Equation (2), leads to a *closed* set of *linear* first order equations for the mean values of the observables

$$i\hbar\left(d\left\langle X_j\right\rangle/dt\right)=i\hbar\left(dTr\left(\rho X_j\right)/dt\right)=\Sigma_k L_{jk}\left\langle X_k\right\rangle \tag{13}$$

where the Liouvillian is $L_{jk}=\sum_i h_i C_{ji}^k=\sum_i h_i\left(\mathbf{M}_j\right)_{ki}$ and our aim is to solve for the mean values for the set of given $\left\{h_i\right\}$'s. For the Hamiltonian of the hardware and when the size dispersion is small, the solution for the $\left\langle X_j\right\rangle$'*s* as a function of time can be read from the experimental maps for different values of *t* along T_2.

The Lie-algebraic time evolution

We make the key assumption that the target can be described in the same *N* dimensional Hilbert space that is used for the hardware. We take *N* to be as large as practical for the hardware and so the Hilbert space is large. When the Hamiltonian matrix is *N* by *N* dimensional the corresponding Liouville matrix is N^2 by N^2 dimensional. The notation is simplified by the definition $\mathbb{N}\equiv N^2$ as above. The Hamiltonian for the target is written as $\hat{H}=\sum_{i=1}^{\mathbb{N}} h_i\hat{X}_i$ with the same set of observables as for the hardware. In other words the set of $\mathbb{N}$ observables is closed under commutation with the Hamiltonian. It is therefore guaranteed, see Wei and Norman(45, 46) for detailed examples, that there is an N^2 by N^2 dimensional time dependent dynamical correlation

matrix Ξ . It replaces solving numerically the Heisenberg equations of motion for the observables, equations (12)

$$\hat{X}_i(t) \equiv U(t)\hat{X}_i U^{\dagger}(t) = \sum_{k=1}^{\mathbb{N}} \Xi_{ik}(t)\hat{X}_k \tag{14}$$

A simple example for N =2 is worked out below.

The Lie algebraic integrated relation (14) is at the heart of surprisal analysis(47) . To make the connection explicit start with an initial state $\rho(0) = \exp\left(-\sum_i \lambda_i(0) X_i(0)\right)$. The surprisal at time t can then be written exactly in terms of the Heisenberg operators at time t, $I(t) = -\ln \rho(t) = -U \ln \rho(0) U^{\dagger} = \sum_i \lambda_i(0) X_i(t)$. Using equation (13) one can rewrite the surprisal at time t as

$$I(t) = \sum_i \lambda_i(0) X_i(t) = \sum_i \lambda_i(0) \sum_j \Xi_{ij}(t) X_j(0) = \sum_j \lambda_j(t) X_j(0) \tag{15}$$

It specifies that the Lagrange multipliers change in time contragradiently to that of the constraints $\lambda_j(t) = \sum_i \lambda_i(0) \Xi_{ij}(t)$

An explicit Lie-algebraic solution for a two (and three) level models

The three level system, a ground state and two excited states, with the laser width spanning the energies of the two excited levels, as shown schematically in Fig. S2, is discussed in the SI. Here we show explicit results for the simpler case of a two level system

$$\hat{H}(t) = 0\hat{E}_{11} - E(t)\mu\left(\hat{E}_{12} + \hat{E}_{21}\right) + \alpha \hat{E}_{22} \tag{16}$$

This Hamiltonian conserves the total population $\hat{E}_{11} + \hat{E}_{22}$. Thereby the time correlation matrix, equation (14), can be written as a three by three matrix because we imposed normalization. For our convenience coherences are rewritten as two anti Hermitian variables $\hat{X}_1 = \left(\hat{E}_{12} + \hat{E}_{21}\right)/2i$, and $\hat{X}_2 = \left(\hat{E}_{21} - \hat{E}_{12}\right)/2$. The third variable is $\hat{X}_3 = \left(\hat{E}_{11} - \hat{E}_{22}\right)/2i$ with $2i\hat{X}_3$ as the difference in the populations of the two states. With details given in the SI, the time correlation matrix Ξ, defined in equation (14), is for these three observables.

$$\begin{pmatrix} X_1(t) \\ X_2(t) \\ X_3(t) \end{pmatrix} = \begin{pmatrix} 1 & 0 & \sin(g_2(t)) \\ 0 & \cos(g_1(t)) & -\cos(g_2(t))\sin(g_1(t)) \\ 0 & \sin(g_1(t)) & \cos(g_2(t))\cos(g_1(t)) \end{pmatrix} \begin{pmatrix} X_1(0) \\ X_2(0) \\ X_3(0) \end{pmatrix} \quad (17)$$

Note that the time correlation matrix, Ξ is real. The functions $g_i(t), i = 1,2$ are obtained from the expansion coefficients of the Hamiltonian, equation (16) , and are derived explicitly in the SI. A numerical example of the evolution of the observables when initially the two state system is in its ground state is shown in figure 3.

Concluding remarks

Quantum processors are expected to build on the unique principles of quantum mechanics to make major improvements in the capabilities of information processing and computing. Here we discussed a design that is based on a multilayered assembly of dimers of quantum dots. The coherences between the states of the quantum dot dimers are our logic variables. We described the dynamical response of such a device and furthermore ask if it can emulate the dynamics of other systems. The input is by nonlinear optical spectroscopy on an ensemble of dots and one reading of the device generates the entire output of interest. The output can be arranged as a matrix. Singular Value Decomposition, SVD, relates the output to a smaller set of hidden principal components. The output can be modified by changing the parameters of the spectroscopy that generates the input. A Lie algebraic discussion of the dynamics of the hardware of N=3 levels is provided in the SI with complete explicit details of the $\mathbb{N} = N^2 = 9$ coherences (= observables) and the resulting 9 by 9 sparse matrices $\mathbf{M}_j, j = 1,2,..,\mathbb{N}$ one matrix per observables, see the SI for explicit results for different operator representation of the SU(3) Lie algebra. Already the simple N=2 model outlined above shows the quantum advantage of our approach. The point is that the time correlation matrix, Ξ, has the dimensions N^2 by N^2 or $(N\text{-}1)^2$ by $(N\text{-}1)^2$ when we impose conservation of populatoins. The Lie algebraic approach leads to a factorization of the Liouvillian into a term that depends only on the structure constants of the Lie algebra gathered into the $\mathbf{M}_j, j = 1,2,..,\mathbb{N}$ matrices and a term that depends on the Hamiltonian. The $\mathbf{M}_j$ matrices are common to the

hardware and the system to be emulated. This factorization allows for emulating the dynamics of a wide class of targeted systems provided that they belong to the same Lie algebra as the hardware.

Acknowledgements

The work of FR is supported by the Fonds National de la Recherche, F.R.S. – FNRS (Belgium), #T.0205.20.

References

1. J. Yuen-Zhou, J. J. Krich, I. Kassal, A. S. Johnson, A. Aspuru-Guzik (2014) Ultrafast Spectroscopy. in *Quantum information and wavepackets* (IOP Publishing, Bristol).
2. E. Collini, 2D Electronic Spectroscopic Techniques for Quantum Technology Applications. *J. Phys. Chem. C* **125**, 13096-13108 (2021).
3. S. Mukamel, *Principles of Nonlinear Optical Spectroscopy* Oxford Series in Optical and Imaging Sciences (Oxford University Press, 1995).
4. P. Brumer, M. Shapiro, Coherence chemistry: controlling chemical reactions [with lasers]. *Acc. Chem. Res.* **22**, 407-413 (1989).
5. J. D. Hybl, A. W. Albrecht, S. M. Gallagher Faeder, D. M. Jonas, Two-dimensional electronic spectroscopy. *Chem. Phys. Lett.* **297**, 307-313 (1998).
6. M. D. Fayer, Dynamics of Liquids, Molecules, and Proteins Measured with Ultrafast 2D IR Vibrational Echo Chemical Exchange Spectroscopy. *Ann. Rev. Phys. Chem.* **60**, 21-38 (2009).
7. P. Hamm, M. T. Zanni, *Concepts and Methods of 2D Infrared Spectroscopy* (Cambridge University Press, Cambridge, 2011).
8. A. Gelzinis, R. Augulis, V. Butkus, B. Robert, L. Valkunas, Two-dimensional spectroscopy for non-specialists. *Biochimica et Biophysica Acta (BBA) - Bioenergetics* **1860**, 271-285 (2019).
9. F. D. Fuller, J. P. Ogilvie, Experimental Implementations of Two-Dimensional Fourier Transform Electronic Spectroscopy. *Ann. Rev. Phys. Chem.* **66**, 667-690 (2015).
10. A. M. Brańczyk, D. B. Turner, G. D. Scholes, Crossing disciplines - A view on two-dimensional optical spectroscopy. *Annalen der Physik* **526**, 31-49 (2014).
11. G. D. Scholes, G. R. Fleming, L. X. Chen, A. Aspuru-Guzik, A. Buchleitner, D. F. Coker, G. S. Engel, R. van Grondelle, A. Ishizaki, D. M. Jonas, J. S. Lundeen, J. K. McCusker, S. Mukamel, J. P. Ogilvie, A. Olaya-Castro, M. A. Ratner, F. C. Spano, K. B. Whaley, X. Zhu, Using coherence to enhance function in chemical and biophysical systems. *Nat.* **543**, 647-656 (2017).
12. Y. Kim, F. Bertagna, E. M. D'Souza, D. J. Heyes, L. O. Johannissen, E. T. Nery, A. Pantelias, A. Sanchez-Pedreño Jimenez, L. Slocombe, M. G. Spencer, J. Al-Khalili, G. S. Engel, S. Hay, S. M. Hingley-Wilson, K. Jeevaratnam, A. R. Jones, D. R. Kattnig, R. Lewis, M. Sacchi, N. S. Scrutton, S. R. P. Silva, J. McFadden, Quantum Biology: An Update and Perspective. *Quantum Reports* **3** (2021).
13. E. Collini, H. Gattuso, Y. Kolodny, L. Bolzonello, A. Volpato, H. T. Fridman, S. Yochelis, M. Mor, J. Dehnel, E. Lifshitz, Y. Paltiel, R. D. Levine, F. Remacle, Room-Temperature Inter-Dot Coherent Dynamics in Multilayer Quantum Dot Materials. *J. Phys. Chem. C* **124**, 1622-16231 (2020).
14. E. Collini, H. Gattuso, R. D. Levine, F. Remacle, Ultrafast fs coherent excitonic dynamics in CdSe quantum dots assemblies addressed and probed by 2D electronic spectroscopy. *J. Chem. Phys.* **154**, 014301 (2021).
15. J. R. Hamilton, E. Amarotti, C. N. Dibenedetto, M. Striccoli, R. D. Levine, E. Collini, F. Remacle, Harvesting a Wide Spectral Range of Electronic Coherences with Disordered Quasi-Homo Dimeric Assemblies at Room Temperature. *Advanced Quantum Technologies* **n/a**, 2200060 (2022).
16. H. Gattuso, R. D. Levine, F. Remacle, Massively parallel classical logic via coherent dynamics of an ensemble of quantum systems with dispersion in size. *Proc. Natl. Acad. Sci. USA* **117**, 21022 (2020).

17. M. A. Nielsen, I. L. Chuang, *Quantum Computation and Quantum Information* (Cambridge University Press, Cambridge, 2010).
18. G. Carleo, I. Cirac, K. Cranmer, L. Daudet, M. Schuld, N. Tishby, L. Vogt-Maranto, L. Zdeborová, Machine learning and the physical sciences. *Rev. Mod. Phys.* **91**, 045002 (2019).
19. J. Biamonte, P. Wittek, N. Pancotti, P. Rebentrost, N. Wiebe, S. Lloyd, Quantum machine learning. *Nat.* **549**, 195-202 (2017).
20. M. Sajjan, J. Li, R. Selvarajan, S. H. Sureshbabu, S. S. Kale, R. Gupta, V. Singh, S. Kais, Quantum machine learning for chemistry and physics. *Chem. Soc. Rev.* **51**, 6475-6573 (2022).
21. Y. Chi, J. Huang, Z. Zhang, J. Mao, Z. Zhou, X. Chen, C. Zhai, J. Bao, T. Dai, H. Yuan, M. Zhang, D. Dai, B. Tang, Y. Yang, Z. Li, Y. Ding, L. K. Oxenløwe, M. G. Thompson, J. L. O'Brien, Y. Li, Q. Gong, J. Wang, A programmable qudit-based quantum processor. *Nat. Commun* **13**, 1166 (2022).
22. C. Reimer, S. Sciara, P. Roztocki, M. Islam, L. Romero Cortés, Y. Zhang, B. Fischer, S. Loranger, R. Kashyap, A. Cino, S. T. Chu, B. E. Little, D. J. Moss, L. Caspani, W. J. Munro, J. Azaña, M. Kues, R. Morandotti, High-dimensional one-way quantum processing implemented on d-level cluster states. *Nat. Phys.* **15**, 148-153 (2019).
23. H.-H. Lu, Z. Hu, M. S. Alshaykh, A. J. Moore, Y. Wang, P. Imany, A. M. Weiner, S. Kais, Quantum Phase Estimation with Time-Frequency Qudits in a Single Photon. *Advanced Quantum Technologies* **3**, 1900074 (2020).
24. J. A. Gyamfi, Fundamentals of quantum mechanics in Liouville space. *European Journal of Physics* **41**, 063002 (2020).
25. E. J. Heller, Time-dependent approach to semiclassical dynamics. *J. Chem. Phys.* **62**, 1544-1555 (1975).
26. D. J. Tannor, *Introduction to quantum mechanics. A time-dependent perspective* (University Science Book, Sausalito, 2007).
27. E. Collini, H. Gattuso, L. Bolzonello, A. Casotto, A. Volpato, C. N. Dibenedetto, E. Fanizza, M. Striccoli, F. Remacle, Quantum Phenomena in Nanomaterials: Coherent Superpositions of Fine Structure States in CdSe Nanocrystals at Room Temperature. *J. Phys. Chem. C* **123**, 31286-31293 (2019).
28. S. Mueller, S. Draeger, X. Ma, M. Hensen, T. Kenneweg, W. Pfeiffer, T. Brixner, Fluorescence-Detected Two-Quantum and One-Quantum–Two-Quantum 2D Electronic Spectroscopy. *J. Phys. Chem. Lett.* **9**, 1964-1969 (2018).
29. L. Bolzonello, F. Bernal-Texca, L. G. Gerling, J. Ockova, E. Collini, J. Martorell, N. F. van Hulst, Photocurrent-Detected 2D Electronic Spectroscopy Reveals Ultrafast Hole Transfer in Operating PM6/Y6 Organic Solar Cells. *J. Phys. Chem. Lett.* **12**, 3983-3988 (2021).
30. K. J. Karki, J. R. Widom, J. Seibt, I. Moody, M. C. Lonergan, T. Pullerits, A. H. Marcus, Coherent two-dimensional photocurrent spectroscopy in a PbS quantum dot photocell. *Nat. Commun* **5**, 5869 (2014).
31. A. A. Bakulin, C. Silva, E. Vella, Ultrafast Spectroscopy with Photocurrent Detection: Watching Excitonic Optoelectronic Systems at Work. *J. Phys. Chem. Lett.* **7**, 250-258 (2016).
32. R. P. Feynman, Simulating physics with computers. *Int. J. Theor. Phys.* **21**, 467-488 (1982).
33. J. Yuen-Zhou, J. J. Krich, M. Mohseni, A. Aspuru-Guzik, Quantum state and process tomography of energy transfer systems via ultrafast spectroscopy. *Proc. Natl. Acad. Sci. USA* **108**, 17615-17620 (2011).
34. B. Fresch, D. Hiluf, E. Collini, R. D. Levine, F. Remacle, Molecular decision trees realized by ultrafast electronic spectroscopy. *Proc. Natl. Acad. Sci. USA* **110**, 17183-17188 (2013).

35. K. Komarova, H. Gattuso, R. D. Levine, F. Remacle, Quantum Device Emulates the Dynamics of Two Coupled Oscillators. *J. Phys. Chem. Lett.* **11**, 6990-6995 (2020).
36. K. Komarova, H. Gattuso, R. D. Levine, F. Remacle, Parallel Quantum Computation of Vibrational Dynamics. *Front. Phys.* **8**, 486 (2020).
37. H. Li, A. D. Bristow, M. E. Siemens, G. Moody, S. T. Cundiff, Unraveling quantum pathways using optical 3D Fourier-transform spectroscopy. *Nat. Commun* **4**, 1390-1390 (2013).
38. J. C. Light, T. Carrington Jr, "Discrete-Variable Representations and their Utilization" in Advances in Chemical Physics. (2000), https://doi.org/10.1002/9780470141731.ch4, pp. 263-310.
39. G. H. Golub, V. Pereyra, The Differentiation of Pseudo-Inverses and Nonlinear Least Squares Problems Whose Variables Separate. *SIAM Journal on Numerical Analysis* **10**, 413-432 (1973).
40. F. Remacle, S. A. Goldstein, D. R. Levine, Multivariate Surprisal Analysis of Gene Expression Levels. *Entropy* **18**, 445 (2017).
41. G. H. Golub, C. F. V. Loan, *Matrix Computations* (John Hopkins University Press, Baltimore, 2013).
42. G. H. Golub, C. Reinsch, "Singular Value Decomposition and Least Squares Solutions" in Linear Algebra, J. H. Wilkinson, C. Reinsch, F. L. Bauer, Eds. (Springer Berlin Heidelberg, Berlin, Heidelberg, 1971), 10.1007/978-3-662-39778-7_10, pp. 134-151.
43. F. Remacle, N. Kravchenko-Balasha, A. Levitzki, R. D. Levine, Information-Theoretic Analysis of Phenotype Changes in Early Stages of Carcinogenesis. *Proc. Natl. Acad. Sci. USA* **107**, 10324-10329 (2010).
44. R. W. Hendler, R. I. Shrager, Deconvolutions based on singular value decomposition and the pseudoinverse: a guide for beginners. *Journal of Biochemical and Biophysical Methods* **28**, 1-33 (1994).
45. J. Wei, E. Norman, Lie Algebraic Solution of Linear Differential Equations. *J. Math. Phys.* **4**, 575-581 (1963).
46. J. Wei, E. Norman, On Global Representations of the Solutions of Linear Differential Equations as a Product of Exponentials. *Proc. Am. Math. So.* **15**, 327-334 (1964).
47. Y. Alhassid, R. D. Levine, Connection between the maximal entropy and the scattering theoretic analyses of collision processes. *Phys. Rev. A* **18**, 89-116 (1978).

Figure Legends

Figure 1: (a) The sequence of 3 pulses used in a BoxCARS measurement and the 3 time intervals. (b) The generation of the polarization cube, measured as a function of the time intervals (left) as shown in (a). After Fourier transformation of the T_1 and the T_3 axis (right), (15) , the cube is converted, (c) to a series of N_{T_3} by N_{T_1} frequency maps at N_{T_2} successive values of T_2. (c) Scheme of the vectorization of the frequency maps. Each map is converted to a column vector and these vectors are arranged as N_{T_2} columns of a matrix **A** of N_{T_3} by N_{T_1} rows.

Figure 2 : (a) The ten largest singular values on a log scale with a plot of the 50 largest ones shown as an insert. (b) The 8 band level structure of the eigenstates of the dimer, adapted from ref. (36) .

Figure 3. The time evolution of the mean values, $< i\hat{X}_k >$ of the three Hermitian observables, iX_1 , iX_2 and iX_3 computed from equation (17). Also shown is time profile of the electric field of the Gaussian optical pulse used for excitation. The parameters of the Hamiltonian (equation 16) are α = 2.18 eV, μ = 0.5 Debye, the electric field envelope of the pulse is confined in a Gaussian envelope, $E(t) = E_0 \exp\left(-(t-t_0)^2 / 2\sigma^2\right)\cos(\omega t)$, with σ =2.49 fs, E_0 = 0.01 a.u (peak intensity of 3.51 10^{12} W/cm^2) and a slightly detuned frequency of ω =2.20 eV.

Supplementary Information

A Quantum Information Processing Machine for Computing by Observables

F. Remacle[1,2], R. D. Levine[2,3*]

[1] Theoretical Physical Chemistry, University of Liège, 4000 Liège, Belgium

[2] The Fritz Haber Research Center for Molecular Dynamics, The Hebrew University of Jerusalem, 91904 Jerusalem, Israel

[3] Department of Chemistry and Biochemistry and Department of Molecular and Medical Pharmacology, David Geffen School of Medicine, University of California, Los Angeles, CA 90095, USA

We process information through the change in time of observables that form a closed Lie algebra, equation (8) of the main text

$$\left[\hat{X}_j,\hat{X}_i\right]=\sum_k^{\mathbb{N}} C_{ji}^k \hat{X}_k$$

The coefficients C_{ji}^k are the structure constants of the algebra. For a quantum system of N states a complete set of such observables in the N^2 coherences of the form $E_j=\left|\alpha\right\rangle\left\langle\beta\right|$ where $\left|\alpha\right\rangle$ and $\left\langle\beta\right|$ are respectively a ket and a bra from the set of N basis states. In terms of N by N matrices, this operator is a matrix that has the entry 1 in row α and in column β and has entries that equal zero elsewhere. The dynamics are described by a Hamiltonian that is a linear sum of the observables, equation (9) of the main text

$$\hat{H}=\sum_i^{\mathbb{N}} h_i\hat{X}_i$$

The $N^2=\mathbb{N}$ coefficients h_i in such an expansion define the specific system of interest.

An essential point is that because the commutator of two observables is a linear combination of observables, equation (8) of the main text, the observables are closed under commutation with the Hamiltonian. This leads to the considerable simplification of the Heisenberg equation of motion for the observables: At any time t the time dependent observable in the Heisenberg picture is a linear combination of the time independent observables, equation (14) of the main text. We discussed the factorization of the dynamics into a term that is a property of the algebra times a term that is special for the Hamiltonian of interest, equation (11) of the main text, repeated here

$$i\hbar\frac{dX_j}{dt}=\left[X_j,H\right]\equiv\sum_k L_{jk}X_k=\sum_i h_i\sum_k C_{ji}^k X_k=\left(\mathbf{h}^T\mathbf{M}_j\right)\cdot\mathbf{X} \qquad \text{(S1)}$$

In the equation of motion the Liouvillian operator $\left(\mathbf{h}\cdot\mathbf{M}_j\right)$ that displaces the observables in time is the product of the N^2 x N^2 matrix $\mathbf{M}_j$ that is the matrix of the structure constants and as such a property of the algebra only and the vetor **h** of the N^2 components of the Hamiltonian of interest. In this SI we examine the choice of matrices $\mathbf{M}_j$ for different choices of operators of the same algebra, see examples below. It is needed fort convenience because it will define Hermitian observables and can also insure orthogonal observables which is quite useful.(1)

Specifically, there is a matrix $\mathbf{M}_i$ for each observable given by $AdX_i = \mathbf{M}_i$ and an element $\left(\mathbf{M}_i\right)_{kj} = c_{ij}^k$.

Explicit Lie Algebraic solutions for a two level system

The simplest case is a two level system with a Hamiltonian

$$H(t) = \begin{pmatrix} 0 & -E(t)\mu \\ -E(t)\mu & \alpha \end{pmatrix}$$

$$\hat{H}(t) = 0\hat{E}_{11} - E(t)\mu\left(\hat{E}_{12} + \hat{E}_{21}\right) + \alpha\hat{E}_{22} \tag{S2}$$

A different basis of three linearly independent operators are the Pauli matrices (divided by 2i):

$$\hat{X}_1 = \frac{1}{2i}\left(\hat{E}_{12} + \hat{E}_{21}\right)\ \hat{X}_2 = \frac{1}{2}\left(\hat{E}_{21} - \hat{E}_{12}\right)\ \ \hat{X}_3 = \frac{1}{2i}\left(\hat{E}_{11} - \hat{E}_{22}\right) \tag{S3}$$

These operators satisfy a cyclic property for the commutators:

$$\left[\hat{X}_1, \hat{X}_2\right] = \frac{}{4i}\left[\left(\hat{E}_{12} + \hat{E}_{21}\right), \left(\hat{E}_{21} - \hat{E}_{12}\right)\right] =$$

$$= \frac{1}{4i}\left(\hat{E}_{11} - \hat{E}_{22} - \hat{E}_{22} + \hat{E}_{11}\right) = \frac{}{2i}\left(\hat{E}_{11} - \hat{E}_{22}\right) = \hat{X}_3$$

$$\left[\hat{X}_2, \hat{X}_3\right] = \frac{1}{4i}\left[\left(\hat{E}_{21} - \hat{E}_{12}\right), \left(\hat{E}_{11} - \hat{E}_{22}\right)\right] = \frac{1}{4i}\left(\hat{E}_{21} + \hat{E}_{21} + \hat{E}_{12} + \hat{E}_{12}\right)$$

$$= \frac{1}{2i}\left(\hat{E}_{12} + \hat{E}_{21}\right) = \hat{X}_1$$

$$\left[\hat{X}_3, \hat{X}_1\right] = -\frac{1}{4}\left[\left(\hat{E}_{11} - \hat{E}_{22}\right), \left(\hat{E}_{12} + \hat{E}_{21}\right)\right] =$$

$$\frac{-1}{4}\left(\hat{E}_{12} - \hat{E}_{21} + \hat{E}_{12} - \hat{E}_{21}\right) = \frac{-1}{2}\left(\hat{E}_{12} - \hat{E}_{21}\right) = \hat{X}_2$$

In matrix notation

$$AdX_1 = \begin{pmatrix} 0 & 0 & 0 \\ 0 & 0 & -1 \\ 0 & 1 & 0 \end{pmatrix}\ AdX_2 = \begin{pmatrix} 0 & 0 & 1 \\ 0 & 0 & 0 \\ -1 & 0 & 0 \end{pmatrix}\ AdX_3 = \begin{pmatrix} 0 & -1 & 0 \\ 1 & 0 & 0 \\ 0 & 0 & 0 \end{pmatrix}$$

To derive the equation (13) of the main text and parametrize the evolution operator a-la Wei-Norman,(2-4) we derive the expressions of the exponentials of the AdX_i's. The three operators are anti-Hermitian, so that the three observables are defined as $i\hat{X}_1$, $i\hat{X}_2$ and $i\hat{X}_3$. This choice, which may appear counter-intuitive, leads however to a numerically more straightforward Wei-Norman parametrization of the evolution operator, as we show below.

The expressions of the exponentials of the AdX_i's are

$$\exp\left(g_1 AdX_1\right)X_1 = X_1$$

$$\exp\left(g_1 AdX_1\right)X_2 = X_2 + \frac{g_1^2}{2!}\underbrace{\left[X_1, X_3\right]}_{(-X_2)} - \frac{g_1^4}{4!}\underbrace{\left[X_1, X_3\right]}_{(-X_2)} + \frac{g_1^6}{6!}\underbrace{\left[X_1, X_3\right]}_{(-X_2)} + \ldots$$

$$+ g_1\underbrace{\left[X_1, X_2\right]}_{X_3} - \frac{g_1^3}{3!}\underbrace{\left[X_1, X_2\right]}_{X_3} + \frac{g_1^5}{5!}\underbrace{\left[X_1, X_2\right]}_{X_3} + \ldots$$

$$= \cos\left(g_1\right)X_2 + \sin\left(g_2\right)X_3$$

$$\exp\left(g_1 AdX_1\right)X_3 = X_3 - \frac{g_1^2}{2!}\underbrace{\left[X_1, X_2\right]}_{X_3} + \frac{g_1^4}{4!}\underbrace{\left[X_1, X_2\right]}_{X_3} - \frac{g_1^6}{6!}\underbrace{\left[X_1, X_2\right]}_{X_3}$$

$$+ g_1\underbrace{\left[X_1, X_3\right]}_{-X_2} - \frac{g_1^3}{3!}\underbrace{\left[X_1, X_3\right]}_{-X_2} + \frac{g_1^5}{5!}\underbrace{\left[X_1, X_3\right]}_{-X_2} - \ldots$$

$$= \cos\left(g_1\right)X_3 - \sin\left(g_1\right)X_2$$

$$\exp\left(g_1 AdX_2\right)X_3 = X_3 + \frac{g_1^2}{2!}\underbrace{\left[X_2, X_1\right]}_{-X_3} - \frac{g_1^4}{4!}\underbrace{\left[X_2, X_1\right]}_{-X_3} + \frac{g_1^6}{6!}\underbrace{\left[X_2, X_1\right]}_{-X_3}$$

$$+ g_1\underbrace{\left[X_2, X_3\right]}_{X_1} - \frac{g_1^3}{3!}\underbrace{\left[X_2, X_3\right]}_{X_1} + \frac{g_1^5}{5!}\underbrace{\left[X_2, X_3\right]}_{X_1} - \ldots$$

$$= \cos\left(g_1\right)X_3 + \sin\left(g_1\right)X_1$$

and similarly for g_2. We can then build the time correlation matrix

$$\Xi(t) = \begin{pmatrix} 1 & 0 & \sin\left(g_2\right) \\ 0 & \cos\left(g_1\right) & -\cos\left(g_2\right)\sin\left(g_1\right) \\ 0 & \sin\left(g_1\right) & \cos\left(g_2\right)\cos\left(g_1\right) \end{pmatrix} \tag{S4}$$

where the first column is $\exp\left(g_1 AdX_1\right)X_1$, the second $\exp\left(g_1 AdX_1\right)X_2$ and the third $\exp\left(g_1 AdX_1\right)\exp\left(g_2 AdX_2\right)X_3$

To derive the equations of motion for the g's we parametrize the evolution operator in product form a-la Wei and Norman

$$U(t)=\exp\left(g_1(t)X_1\right)\exp\left(g_2(t)X_2\right)...\exp\left(g_l(t)X_l\right) \tag{S5}$$

Then for dU/dt , we have

$$i\frac{dU}{dt}=i\sum_i^l g_i'(t)\left(\prod_{j=1}^{i-1}\exp\left(g_jX_j\right)\right)X_i\left(\prod_{j=i}^{l}\exp\left(-g_jX_j\right)\right) \tag{S6}$$

and

$$HU(t)=\left(\sum_{i=1}^{l}h_i(t)X_i\right)U(t) \tag{S7}$$

so by multiplying by $U^{-1}(t)$ on right we get

$$\begin{aligned}\sum_{i=1}^{l}h_i(t)X_i&=i\sum_{i=1}^{l}g_i'(t)\left(\prod_{j=1}^{i-1}\exp\left(g_jX_j\right)\right)X_i\left(\prod_{j=i-1}^{1}\exp\left(-g_jX_j\right)\right)\\&=i\sum_{i=1}^{l}g_i'(t)\left(\prod_{j=1}^{i-1}\exp\left(g_jadX_j\right)\right)X_i\end{aligned} \tag{S8}$$

and thereby one has a matrix equation for the rate of change of the g's, denoted by a prime $g_i'(t)$:

$$\sum_{k=1}^{l}h_k(t)X_k=i\sum_{i=1}^{l}\sum_{k=1}^{l}g_i'(t)\xi_i^k\left(g_1(t)...g_l(t)\right)X_k \tag{S9}$$

Defining the time correlation matrix Ξ with elements $\Xi_{ik}=\xi_i^k(t)$ we have:

$$d\mathbf{g}/dt=\mathbf{g}'(t)=\Xi^{-1}\,\mathbf{h} \tag{S10}$$

Note that the matrix Ξ is real.

For the 2 level system with the set of 3 observables defined in Eq.(s3), using Eq.(S4), we have an analytical expression for Ξ^{-1} which leads to:

$$\begin{pmatrix}g_1'\\g_2'\\g_3'\end{pmatrix}=\begin{pmatrix}1&\sin g_1(t)\tan g_2(t)&-\cos g_1(t)\tan g_2(t)\\0&\cos g_1(t)&\sin g_1(t)\\0&-\sec g_2(t)\sin g_1(t)&\cos g_1(t)\sec g_2(t)\end{pmatrix}\begin{pmatrix}-2E(t)\mu\\0\\-\alpha\end{pmatrix} \tag{S11}$$

Plots of the g's as a function of time for the two coherences of the example in the main text are shown in Figure S1. They are computed by numerical integration of equation (S11).

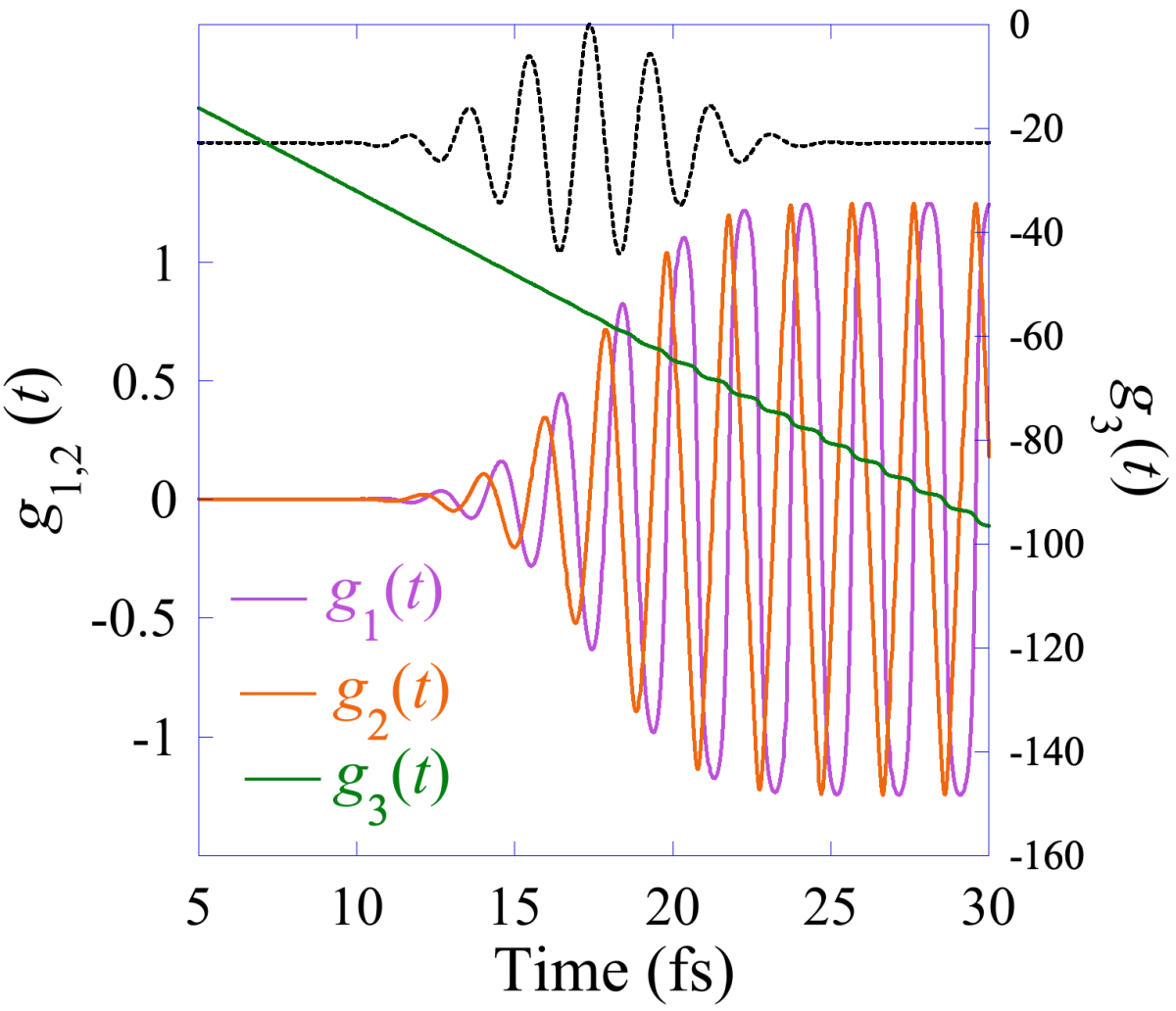

Figure S1. Plot of $g_1(t)$ $g_2(t)$ and $g_3(t)$ as well as of the electric field time profile of the pulse, $E(t) = E_0 \exp\left(-(t-t_0)^2 / 2\sigma^2\right)\cos(\omega t)$ scaled for an easier reading, with σ =2.49 fs, E_0 = 0.01 a.u (peak intensity of 3.51 10^{12} W/cm^2) and a slightly detuned frequency of ω =2.20 eV.

Results for the time correlation matrix function that governs the change in the observables with time are given in equation 17 of the main text with numerical results shown in figure 4.

Explicit solution of the three level system

The three level system, a ground state and two excited states, with the laser width spanning the energies of the two excited levels, as shown schematically in Fig. S2

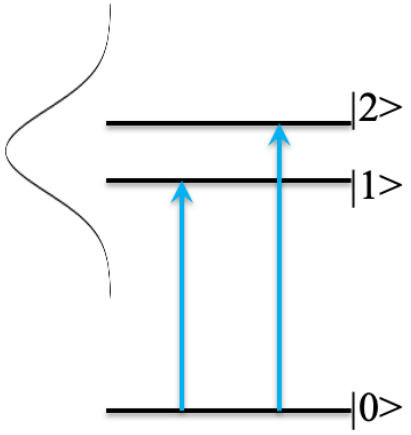

Figure S2: Scheme of the excitation level for a system with two excited states.

There are nine E_{ij} operators but only 8 are linearly independent because of the constraint of normalization, $\hat{I} = \sum_i \hat{E}_{ii}$. The Hamiltonian of the hardware is

$$\hat{H}'(t) = \hat{H}_0 - E(t)\cdot\hat{\mu} = \alpha_2\hat{E}_{22} + \alpha_3\hat{E}_{33} - E(t)\mu_{12}\left(\hat{E}_{12} + \hat{E}_{21}\right) - E(t)\mu_{13}\left(\hat{E}_{13} + \hat{E}_{31}\right) \qquad \text{(S12)}$$

$\hat{H}_0$ is diagonal with α_2 and α_3 as the two excited state energies while the full Hamiltonian is a somewhat sparse 3 by 3 matrix:

$$\hat{H}'(t) = \begin{pmatrix} 0 & -E(t)\mu_{12} & -E(t)\mu_{13} \\ -E(t)\mu_{12} & \alpha_2 & 0 \\ -E(t)\mu_{13} & 0 & \alpha_3 \end{pmatrix} \qquad (13)$$

The commutation relations, written in the algebraic 'ad' notation are

$$\begin{aligned} ad_{ij}\hat{E}_{kl} &\equiv \left[\hat{E}_{ij}, \hat{E}_{kl}\right] = \hat{E}_{il}\delta_{jk} - \hat{E}_{kj}\delta_{li} \\ ad_{ij}^2\hat{E}_{kl} &= \left[\hat{E}_{ij}, \left[\hat{E}_{ij}, \hat{E}_{kl}\right]\right], ...etc \end{aligned} \qquad \text{(S14)}$$

For example

$$ad_{ik}\hat{E}_{il} = \left[E_{ik}, E_{il}\right] = 0, \quad ad_{ij}\hat{E}_{kj} = 0, .. \qquad \text{(S15)}$$

Some commutators are not zero while higher order ones are, for example

$$ad_{ij}\hat{E}_{ji} = \hat{E}_{ii} - \hat{E}_{jj}, \; ad_{ij}^2\hat{E}_{ji} = ad_{ij}\hat{E}_{ii} - ad_{ij}\hat{E}_{jj} = -2\hat{E}_{ij}, \; ad_{ij}^3\hat{E}_{ji} = -\left[\hat{E}_{ij}, \hat{E}_{ij}\right] = 0 \qquad \text{(S16)}$$

A basis analogous(5) to that used for two levels but using Hermitian operators is

$$\lambda_1 = \begin{pmatrix} 0 & 1 & 0 \\ 1 & 0 & 0 \\ 0 & 0 & 0 \end{pmatrix} = E_{12} + E_{21} \ , \ \lambda_2 = \begin{pmatrix} 0 & -i & 0 \\ i & 0 & 0 \\ 0 & 0 & 0 \end{pmatrix} = -iE_{12} + iE_{21} \ ,$$

$$\lambda_3 = \begin{pmatrix} 1 & 0 & 0 \\ 0 & -1 & 0 \\ 0 & 0 & 0 \end{pmatrix} = E_{11} - E_{22}$$

$$\lambda_4 = \begin{pmatrix} 0 & 0 & 1 \\ 0 & 0 & 0 \\ 1 & 0 & 0 \end{pmatrix} = E_{13} + E_{31} , \ \lambda_5 = \begin{pmatrix} 0 & 0 & -i \\ 0 & 0 & 0 \\ i & 0 & 0 \end{pmatrix} = -iE_{13} + iE_{31}$$

$$\lambda_6 = \begin{pmatrix} 0 & 0 & 0 \\ 0 & 0 & 1 \\ 0 & 1 & 0 \end{pmatrix} = E_{23} + E_{32} , \ \lambda_7 = \begin{pmatrix} 0 & 0 & 0 \\ 0 & 0 & -i \\ 0 & i & 0 \end{pmatrix} = -iE_{23} + iE_{32}$$

$$\lambda_8 = \frac{1}{\sqrt{3}} \begin{pmatrix} 1 & 0 & 0 \\ 0 & 1 & 0 \\ 0 & 0 & -2 \end{pmatrix} \text{ or}$$

$$\lambda_8 = \frac{1}{\sqrt{3}} \begin{pmatrix} 1 & 0 & 0 \\ 0 & -1 & 0 \\ 0 & 0 & 0 \end{pmatrix} + \frac{2}{\sqrt{3}} \begin{pmatrix} 0 & 0 & 0 \\ 0 & 1 & 0 \\ 0 & 0 & -1 \end{pmatrix} = \frac{1}{\sqrt{3}} \left(E_{11} - E_{22} \right) + \frac{2}{\sqrt{3}} \left(E_{22} - E_{33} \right)$$

These linearly independent, orthogonal $\left(Tr\left[\lambda_i \lambda_k \right] = 2\delta_{ik} \right)$ and normalized operators satifisfy

$$\left[\lambda_i , \lambda_k \right] = \sum_{l=1}^{N} \ c_{ik}^{l} 2i\lambda_l$$

We can then use formula for the structure coefficients

$$Tr\left(\left[\lambda_i , \lambda_k \right] , \lambda_l \right) = 2i \sum_{m} \ c_{ik}^{m} Tr\left[\lambda_m \lambda_l \right] = 2i \sum_{m} \ c_{ik}^{m} 2\delta_{ml} = 4ic_{ik}^{l}$$

Meaning that the structure coefficients can be calculated as

$$C_{ik}^{m} = \frac{1}{4i} Tr\left(\left[\lambda_i , \lambda_k \right] \lambda_m \right)$$

Using the cyclic invariance of the trace shows that the coefficients are totally antisymmetric

$$4iC_{ik}^{l} = \frac{1}{4i} Tr\left(\left[\lambda_i, \lambda_k\right]\lambda_l\right) = Tr\left(\lambda_i\lambda_k\lambda_l - \lambda_k\lambda_i\lambda_l\right)$$

$$= -Tr\left(\lambda_l\lambda_k\lambda_i - \lambda_l\lambda_i\lambda_k\right) = -Tr\left(\left[\lambda_i, \lambda_k\right]\lambda_l\right) = -4iC_{ki}^{l}$$

This generates a table of the non vanishing structure coefficients of the algebra SU(3).

i	1	1	1	2	2	3	3	4	6
k	2	4	5	4	5	4	6	5	7
l	3	7	6	6	7	5	7	8	8
C_{ik}^{l}	1	1/2	-1/2	1/2	1/2	1/2	-1/2	$3^{1/2}/2$	$3^{1/2}/2$

The resulting matrices **M** are:

$$\mathbf{M}_{\lambda_1} = 2i \begin{pmatrix} 0 & & & & & & & & \\ & 0 & -1 & & & & & & \\ & 1 & 0 & & & & & & \\ & & & 0 & & & -1/2 & & \\ & & & & 0 & 1/2 & & & \\ & & & & -1/2 & 0 & & & \\ & & & 1/2 & & & 0 & & \\ & & & & & & & 0 & \\ & & & & & & & & 0 \end{pmatrix}$$

$$\mathbf{M}_{\lambda_2} = 2i \begin{pmatrix} 0 & & 1 & & & & & & \\ & 0 & & & & & & & \\ -1 & & 0 & & & & & & \\ & & & 0 & & -1/2 & & & \\ & & & & 0 & & -1/2 & & \\ & & & 1/2 & & 0 & & & \\ & & & & 1/2 & & 0 & & \\ & & & & & & & 0 & \\ & & & & & & & & 0 \end{pmatrix}$$

$$\mathbf{M}_{\lambda_3} = 2i \begin{pmatrix} 0 & 1 & & & & & & \\ -1 & 0 & & & & & & \\ & & 0 & & & & & \\ & & & 0 & -1/2 & & & \\ & & & 1/2 & 0 & & & \\ & & & & & 0 & -1/2 & \\ & & & & & 1/2 & 0 & \\ & & & & & & & 0 \end{pmatrix}$$

$$\mathbf{M}_{\lambda_4} = 2i \begin{pmatrix} 0 & & & & & & 1/2 & \\ & 0 & & & & 1/2 & & \\ & & 0 & & 1/2 & & & \\ & & & 0 & & & & \\ & & -1/2 & & 0 & & & -\sqrt{3}/2 \\ & -1/2 & & & & 0 & & \\ 1/2 & & & & & & 0 & \\ & & & \sqrt{3}/2 & & & & 0 \end{pmatrix}$$

$$\mathbf{M}_{\lambda_5} = 2i \begin{pmatrix} 0 & & & & & -1/2 & & \\ & 0 & & & & & 1/2 & \\ & 0 & 0 & & 1/2 & & & \\ & & & 0 & & & & \sqrt{3}/2 \\ & & -1/2 & & 0 & & & \\ 1/2 & & & & & 0 & & \\ & -1/2 & & & & & 0 & \\ & & & -\sqrt{3}/2 & & & & 0 \end{pmatrix}$$

$$\mathbf{M}_{\lambda_6} = 2i \begin{pmatrix} 0 & & & & 1/2 & & & \\ & 0 & & -1/2 & & & & \\ & 0 & 0 & & & -1/2 & & \\ & 1/2 & & 0 & & & & \\ -1/2 & & & & 0 & & & \\ & & & & & 0 & & \\ & & 1/2 & & & & 0 & -\sqrt{3}/2 \\ & & & & & & \sqrt{3}/2 & 0 \end{pmatrix}$$

$$\mathbf{M}_{\lambda_7} = 2i \begin{pmatrix} 0 & & & 1/2 & & & & \\ & 0 & & & -1/2 & & & \\ & & 0 & & & 1/2 & & \\ -1/2 & & & 0 & & & & \\ & 1/2 & & & 0 & & & \\ & & -1/2 & & & 0 & & \sqrt{3}/2 \\ & & & & & & 0 & \\ & & & & & -\sqrt{3}/2 & & 0 \end{pmatrix}$$

$$\mathbf{M}_{\lambda_8} = 2i \begin{pmatrix} 0 & & & & & & & \\ & 0 & & & & & & \\ & & 0 & & & & & \\ & & & 0 & -\sqrt{3}/2 & & & \\ & & & \sqrt{3}/2 & 0 & & & \\ & & & & & 0 & -\sqrt{3}/2 & \\ & & & & & \sqrt{3}/2 & 0 & \\ & & & & & & & 0 \end{pmatrix}$$

By linear combination of the λ 's, one can define a new set of operators of SU (3) that lead to matrices **M** that are not skew symmetric

$$\mathbf{e}^{(T)}{}_1 = -\frac{1}{2} i\lambda_1 \ , \ \mathbf{e}^{(T)}{}_2 = -\frac{1}{2} i\lambda_2 \ , \ \mathbf{e}^{(T)}{}_3 = -\frac{1}{2} i\lambda_3$$

$$\mathbf{e}^{(U)}{}_1 = -\frac{1}{2} i\lambda_6 \ , \ \mathbf{e}^{(U)}{}_2 = -\frac{1}{2} i\lambda_7 \ , \ \mathbf{e}^{(U)}{}_3 = -\frac{1}{4} i\left(-\lambda_3 + \sqrt{3}\lambda_8\right)$$

$$\mathbf{e}^{(V)}{}_1 = -\frac{1}{2} i\lambda_4 ,\ \mathbf{e}^{(V)}{}_2 = -\frac{1}{2} i\lambda_5 ,\ \ \mathbf{e}^{(V)}{}_3 = -\frac{1}{4} i\left(\lambda_3 + \sqrt{3}\lambda_8\right)$$

These obeys the cyclic property of the commutators

$\left[e^{(X)}{}_1, e^{(X)}{}_2\right] = e^{(X)}{}_3$ cyclic in 1,2,3 for X=T, U and V

It follows that there are three subalgebras SU(2).

This third set of operators was proposed in ref. (4) :

$$iH_1 = \begin{pmatrix} 1 & 0 & 0 \\ 0 & -1 & 0 \\ 0 & 0 & 0 \end{pmatrix} = E_{11} - E_{22} \ ,\ iH_2 = \begin{pmatrix} 0 & 0 & 0 \\ 0 & -i & 0 \\ 0 & 0 & i \end{pmatrix} = -iE_{22} + iE_{33} ,$$

$$X_{12} = \begin{pmatrix} 0 & 1 & 0 \\ -1 & 0 & 0 \\ 0 & 0 & 0 \end{pmatrix} = E_{12} - E_{21} ,\ Y_{12} = \begin{pmatrix} 0 & i & 0 \\ i & 0 & 0 \\ 0 & 0 & 0 \end{pmatrix} = iE_{12} + iE_{21}$$

$$X_{13} = \begin{pmatrix} 0 & 0 & 1 \\ 0 & 0 & 0 \\ -1 & 0 & 0 \end{pmatrix} = E_{13} - E_{31} ,\ Y_{13} = \begin{pmatrix} 0 & 0 & i \\ 0 & 0 & 0 \\ i & 0 & 0 \end{pmatrix} = iE_{13} + iE_{31}$$

$$X_{23} = \begin{pmatrix} 0 & 0 & 0 \\ 0 & 0 & 1 \\ 0 & -1 & 0 \end{pmatrix} = E_{23} - E_{32} ,\ \ Y_{23} = \begin{pmatrix} 0 & 0 & 0 \\ 0 & 0 & i \\ 0 & i & 0 \end{pmatrix} = iE_{23} + iE_{32}$$

The structure constants $c_{ij}^k = -c_{ji}^k$ are

$c_{13}^4 = c_{41}^3 = c_{34}^1 = 2$

$c_{15}^6 = c_{61}^5 = c_{56}^1 = 2$

$c_{27}^8 = c_{82}^7 = c_{78}^2 = 2$

$c_{45}^8 = c_{84}^5 = c_{58}^4 = 1$

$c_{46}^7 = c_{74}^6 = c_{67}^4 = -1$

$c_{35}^7 = c_{73}^5 = c_{57}^3 = -1$

$c_{36}^8 = c_{83}^6 = c_{68}^3 = -1$

$c_{17}^8 = c_{81}^7 = -1 ,\ c_{78}^1 = 0$

$c_{23}^4 = c_{42}^3 = -1, \;\; c_{34}^2 = 0$

$c_{25}^6 = c_{62}^5 = 1, \quad c_{56}^2 = 2$

Which leads to the following **M** matrices:

$$\mathbf{M}_1 = \begin{pmatrix} 0 & & & & & & & \\ & 0 & & & & & & \\ & & 0 & c_{14}^3 & & & & \\ & & c_{13}^4 & 0 & & & & \\ & & & & 0 & c_{16}^5 & & \\ & & & & c_{15}^6 & 0 & & \\ & & & & & & 0 & c_{18}^7 \\ & & & & & & c_{17}^8 & 0 \end{pmatrix}, \quad \mathbf{M}_3 = \begin{pmatrix} 0 & & c_{34}^1 & & & & & \\ & 0 & & & & & & \\ & & 0 & & & & & \\ c_{31}^4 & c_{32}^4 & & 0 & & & & \\ & & & & 0 & & c_{37}^5 & \\ & & & & & 0 & & c_{38}^6 \\ & & & & c_{35}^7 & & 0 & \\ & & & & & c_{36}^8 & & 0 \end{pmatrix}$$

$$\mathbf{M}_2 = \begin{pmatrix} 0 & & & & & & & \\ & 0 & & & & & & \\ & & 0 & c_{24}^3 & & & & \\ & & c_{23}^4 & 0 & & & & \\ & & & & 0 & c_{26}^5 & & \\ & & & & c_{25}^6 & 0 & & \\ & & & & & & 0 & c_{27}^8 \\ & & & & & & c_{28}^7 & 0 \end{pmatrix} \quad \mathbf{M}_4 = \begin{pmatrix} 0 & & c_{43}^1 & & & & & \\ & 0 & & & & & & \\ c_{41}^3 & c_{42}^3 & 0 & & & & & \\ & & & 0 & & & & \\ & & & & 0 & & & c_{48}^5 \\ & & & & & 0 & c_{47}^6 & \\ & & & & & c_{46}^7 & 0 & \\ & & & & c_{45}^8 & & & 0 \end{pmatrix}$$

,

,

$$\mathbf{M}_5 = \begin{pmatrix} 0 & & & & c_{56}^{1} & & \\ & 0 & & & c_{56}^{2} & & \\ & & 0 & & & c_{57}^{3} & \\ & & & 0 & & & c_{54}^{8} \\ & & & & 0 & & \\ c_{51}^{6} & c_{52}^{6} & & & 0 & & \\ & & c_{53}^{7} & & & 0 & \\ & & & c_{54}^{8} & & & 0 \end{pmatrix}, \quad \mathbf{M}_6 = \begin{pmatrix} 0 & & & c_{65}^{1} & & & \\ & 0 & & c_{62}^{5} & & & \\ & & 0 & & & & c_{68}^{3} \\ & & & 0 & & c_{64}^{7} & \\ c_{61}^{5} & c_{65}^{2} & & 0 & & & \\ & & & & 0 & & \\ & & & c_{67}^{4} & & 0 & \\ & & c_{63}^{8} & & & & 0 \end{pmatrix}$$

$$\mathbf{M}_7 = \begin{pmatrix} 0 & & & & & & c_{78}^{2} \\ & 0 & & & & & \\ & & 0 & c_{73}^{5} & & & \\ & & & 0 & c_{76}^{4} & & \\ & & c_{75}^{3} & & 0 & & \\ & & & c_{74}^{6} & & 0 & \\ & & & & & & 0 \\ c_{71}^{8} & c_{72}^{8} & & & & & 0 \end{pmatrix}, \quad \mathbf{M}_8 = \begin{pmatrix} 0 & & & & & & \\ & 0 & & & & c_{87}^{2} & \\ & & 0 & & c_{83}^{6} & & \\ & & & 0 & c_{84}^{5} & & \\ & & & c_{85}^{4} & 0 & & \\ & & c_{86}^{3} & & & 0 & \\ c_{81}^{7} & c_{82}^{7} & & & & 0 & \\ & & & & & & 0 \end{pmatrix}$$

References

1. K. Komarova, F. Remacle, R. D. Levine, Compacting the density matrix in quantum dynamics: Singular value decomposition of the surprisal and the dominant constraints for anharmonic systems. *J. Chem. Phys.* **155**, 204110 (2021).
2. J. Wei, E. Norman, Lie Algebraic Solution of Linear Differential Equations. *J. Math. Phys.* **4**, 575-581 (1963).
3. J. Wei, E. Norman, On Global Representations of the Solutions of Linear Differential Equations as a Product of Exponentials. *Proc. Am. Math. So.* **15**, 327-334 (1964).
4. C. Altafini, Parameter differentiation and quantum state decomposition for time varying Schrödiner equations. *Reports on Mathematical Physics* **52**, 381-400 (2003).
5. W. Pfeifer, "The Lie algebras su(N)" in The Lie Algebras su(N): An Introduction, W. Pfeifer, Ed. (Birkhäuser Basel, Basel, 2003), 10.1007/978-3-0348-8097-8_2.